Abstracta

Ano XXIX - N. 02

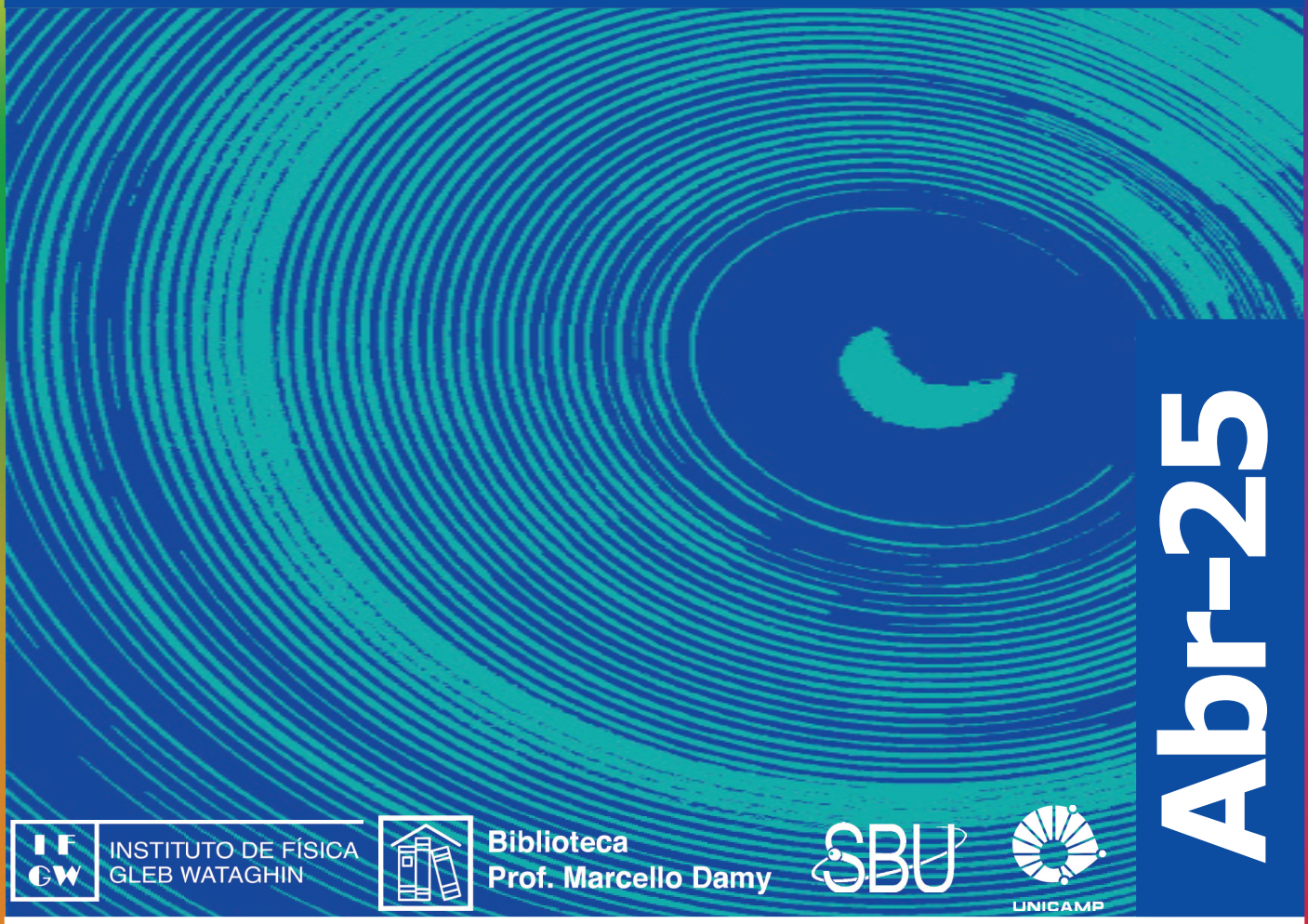

Artigos publicados 2025

P026-2025 à P065-2025

Defesas de Dissertações do IFGW

D006-2025 à D008-2025

Defesas de Teses do IFGW

T005-2025 à T006-2025

Artigos publicados

[P026-2025] "A planar- sheet nongraphitic zero- bandgap sp2 carbon phase made by the low- temperature reaction of γ- graphyne"

Aliev. A. E.; Guo, Y. Z.; **Fonseca, A. F.*; Galvao, D. S.*; Kanegae, G. B.***

The highest sheet symmetry form of graphyne, with one triple bond between each neighboring hexagon in graphene, irreversibly transforms exothermically at ambient pressure and low temperatures into a nongraphitic, planar- sheet, zero- bandgap phase consisting of intrasheet- bonded sp2 carbons. The synthesis of this sp2 carbon phase is demonstrated, and other carbon phases are described for possible future synthesis from graphyne without breaking graphyne bonds. While measurements and theory indicate that the reacting graphyne becomes nonplanar because of sheet wrinkling produced by dimensional mismatch between reacted and nonreacted sheet regions, sheet planarity is regained when the reaction is complete. Although the observed elimination of triple bonds to make parallel planar sp2 carbon sheets likely requires ordered transformation within each sheet, diffraction data for reacted multisheet stacks indicate that the relative lateral positions of neighboring sheets are disordered, as predicted, since no crystalline diffraction peak (other than for the intersheet spacing) is observed.

PROCEEDINGS OF THE NATIONAL ACADEMY OF SCIENCES OF THE UNITED STATES OF AMERICA 122[5], e2413194122, 2025. DOI: 10.1073/pnas.2413194122/-/DCSupplemental

[P027-2025] "Acid Pre-Treatment of Graphite Electrodes: An Alternative to Enhance the Sensing Performance of Benzenediol Isomers"

Silva, C. C. da; Moreto, J. A.; Pereira, J. F. D.; Resende, M. C. S.; **Siervo, A. de***; Nossol, E.; Gelamo, R. V.; Munoz, R. A. A.;

Electroanalytical techniques offer several advantages: low cost, portability, and high analysis frequency. These benefits can be further enhanced by replacing standard electrodes (boron-doped diamond, glassy carbon, gold, platinum, etc.) with abundant, low-cost carbon materials. Pyrolytic Graphite Sheet (GS) electrodes have recently emerged as a reliable alternative, providing good stability, sensitivity, and mechanical strength. Their performance can be improved with acidic treatments. Scanning electron and atomic force microscopy images revealed irregular patterns on the edges of acid-treated GS, consistent with Raman spectra, which showed changes in the ID/IG ratio, indicating more structural defects. The acidic treatment also increased the electroactive area of GS electrodes and oxygen-containing functional groups, as observed by XPS, leading to enhanced signal currents. Additionally, electrochemical impedance spectroscopy confirmed a decrease in charge transfer resistance. Treated electrodes exhibited lower detection limits for catechol (0.58 mu mol l-1) and resorcinol (0.16 mu mol l-1) compared to untreated GS electrodes. The presence of potential interferents, such as KCl, NaCl, glucose, ascorbic acid, ibuprofen, paracetamol, and uric acid, did not affect the detection of catechol and resorcinol. Recovery values for spiked water samples ranged from 80% to 109%, confirming the accuracy of the proposed analytical method. Electroanalytical techniques are cost-effective, portable, and high-frequency.GS electrodes are a reliable, cost-effective alternative to traditional electrodes.Acidic treatment improves GS electrodes stability, sensitivity, and electroactive area.Acidic treatment reduces charge transfer resistance and enhances signal current.Treated GS electrodes show lower detection limits and no interference, ensuring accuracy.

JOURNAL OF THE ELECTROCHEMICAL SOCIETY 172[2], 027505 , 2025. DOI: 10.1149/1945-7111/adafe1

[P028-2025] "Boosting aerosol surface effects: strongly enhanced cooperative surface propensity of atmospherically relevant organic molecular ions in aqueous solution"

Kaur, H.; Thürmer, S.; Gholami, S.; **Pinheiro, J.***; **Brito, A. N. de***

The effects of atmospheric aerosols are key uncertainties in climate models. One reason is the complex aerosol composition which includes a relatively large fraction of organics. Another reason is the small size of aerosols, which makes surface effects and processes important. These two factors make surface-active organics relevant for atmospheric aerosols, as they can affect crucial processes, such as chemical aging and water accommodation, as well as properties such as the surface tension, which drives droplet formation. Two exemplary types of atmospherically relevant organics are carboxylic acids and alkyl amines, and often both are found together within aerosols. In the most atmospherically significant pH range, these exist as alkyl-carboxylate ions and alkyl-ammonium ions. Using liquid-jet photoelectron spectroscopy, tuned to high surface sensitivity, we measured the alkyl-carboxylate anions and the alkyl-ammonium cations of alkyl chain lengths of 1 to 6 carbon atoms, both as single-component and mixed-component aqueous solutions. This enabled us to systematically study how their surface propensity is affected by the length of the alkyl chains and how cooperative ion-ion interactions result in strongly increased surface propensity. An exponential increase in surface propensity is found for the single-species solutions, with cooperative solute-solute effects in mixed solutions of 1 : 1 molar ratio drastically increasing the number of molecules present at the solutions' surfaces up to a factor of several hundred. This cooperative surface propensity is shown to strongly affect the amounts of organics at the surface. These changes can significantly influence radiative forcing via aerosol growth, cloud condensation nuclei activity, and aerosol chemical aging. Our results demonstrate the principal feasibility of a more advanced input of molecular details for creating parameterized descriptions of aerosol surface composition needed to properly account for their impacts in climate models.

ATMOSPHERIC CHEMISTRY AND PHYSICS 25[6], p. 3503-3518, 2025. DOI: 10.5194/acp-25-3503-2025

[P029-2025] "Calibrating the absolute magnitude of type Ia supernovae in nearby galaxies using [O II] and implications for H0"

Dixon, M.; Mould, J.; Lidman, C.; **Sobreira, F.***; et al. DES Collaboration.

The present state of cosmology is facing a crisis where there is a fundamental disagreement in measurements of the Hubble constant (H-0), with significant tension between the early and late Universe methods. Type Ia supernovae (SNe Ia) are important to measuring H-0 through the astronomical distance ladder. However, there remains potential to better standardize SN Ia light curves by using known dependencies on host galaxy properties after the standard light curve width and colour corrections have been applied to the peak SN Ia luminosities. To explore this, we use the 5-yr photometrically identified SNe Ia sample obtained by the Dark Energy Survey, along with host galaxy spectra obtained by the Australian Dark Energy Survey. Using host galaxy spectroscopy, we find a significant trend with the equivalent width (EW) of the [O II] lambda lambda 3727, 29 doublet, a proxy for specific star formation rate, and Hubble residuals. We find that the correlation with [O II] EW is a powerful alternative to the commonly used mass step after initial light--curve corrections. Applying this [O II] EW correction to 20 SNe Ia in calibrator galaxies observed with WiFeS, we examined the impact on SN Ia absolute magnitudes and H-0.Our [O II] EW corrections result in H-0 values ranging between 73.04 and 73.51 kms(-1)Mpc(-1), with a combined statistical and systematic uncertainty of similar to 1.31kms(-1)Mpc(-1).

However, even with this additional correction, the impact of host galaxy properties in standardizing SNe Ia appears limited in reducing the current tension (similar to 5 sigma) with the cosmic microwave background result for H-0.

MONTHLY NOTICES OF THE ROYAL ASTRONOMICAL SOCIETY 538 [2], p. 782-796, 2025. DOI: 10.1093/mnras/staf266

[P030-2025] "Carbon powder from sugarcane bagasse: Controlled synthesis for on-demand H2O2 electrogeneration"

Sperandio, D. C.; Lourenço, J. C.; Nogueira, B.; **Siervo, A. de***

In this study, we developed a green synthesis route to produce a conductive carbon material selective towards H2O2 electrogeneration, utilizing sugarcane bagasse (SCB), an abundant byproduct of the sugar and ethanol industries, as the feedstock. Through a tailored process involving impregnation with phosphoric acid and thermal activation, we synthesized amorphous porous carbon with outstanding properties - a surface area above 1500 m2g-1 and adjustable porosity from meso to micropores. The application of the optimized carbon material in the Gas Diffusion Electrode (GDE) yielded an H2O2 concentration of up to 1900 mg L- 1 in 120 min of electrolysis, even at practical current densities of up to 160 mA cm- 2. The findings of this study point to the suitability of SCBderived carbon material as a sustainable and cost-effective alternative to the traditional petrol-derived carbon materials typically employed in H2O2 electrogeneration; clearly, these findings have promising implications for environmentally conscious practices.

RENEWABLE ENERGY 244, 122715, 2025. DOI: 10.1016/j.renene.2025.122715

[P031-2025] "Characterization of Fe nanoparticles on SrTiO3 (001) using X-ray photoelectron diffraction (XPD)"

Medeiros, Y. S. A.; **Siervo, A. de*; Landers, R.***; Nascente, P. A. P.; Otero, E. P. U.; Back, T.; Pancotti, A.

The perovskite ceramic strontium titanate (SrTiO3 or STO) presents remarkable properties that make it very promising for catalytic, photocatalytic, electronic, magnetic, and spintronic applications. The bulk SrTiO3 crystal consists of alternating TiO2 and SrO layers along the (001) direction, with surfaces terminated by either layer. The deposition of Fe on SrTiO3 (001) can provide Fe nanoparticles of interest for various applications. Adequate characterization of the properties and structures of these nanoparticles and substrate is essential. In this work, the formation and structure of Fe nanoparticles grown on SrTiO3 (001) (/5 x /5)R26.6 degrees surface were characterized by low energy electron diffraction (LEED) and X-ray photoelectron diffraction (XPD). The comparison between experimental and theoretical XPD results involving multiple scattering calculations indicates a coexistence of Fe nanoparticles in both bcc and fcc structures.

VACUUM 238, 114281, 2025. DOI: 10.1016/j.vacuum.2025.114281

[P032-2025] "Comparing dynamics, pinning and ratchet effects for skyrmionium, skyrmions, and antiskyrmions"

Souza, J. C. B.; **Vizarim, N. P.*;** Reichhardt, C. J. O.; Reichhardt, C.; Venegas, P. A.

We compare the driven dynamics of skyrmions, antiskyrmions, and skyrmionium interacting with random disorder, circular defects, and asymmetric potentials. When interacting with a line defect at a constant drive, skyrmions and antiskyrmions show an acceleration effect for motion along the wall and a drop in velocity when they can cross the barrier. In contrast, skyrmionium travels at a reduced velocity when moving along a wall, and exhibits an increase in velocity once it can cross the barrier. For point defects, skyrmionium can be pinned for a finite fixed period of time, while for skyrmions and antiskyrmions, the Magnus force creates a deflection from the defect and an acceleration effect. For a given drive, skyrmionium moves twice as fast as skyrmions; however, skyrmionium is more susceptible to pinning effects than skyrmions and antiskyrmions. Additionally, there is a critical threshold where the skyrmionium transforms to a skyrmion that is associated with a drop in the velocity of the texture. We show that all three textures exhibit diode and ratchet effects when interacting with an asymmetric substrate, but skyrmions and antiskyrmions show a stronger ratcheting effect than skyrmionium due to the Magnus force.

JOURNAL OF PHYSICS-CONDENSED MATTER 37[16], 165801, 2025. DOI: 10.1088/1361-648X/adbba6

[P033-2025] "Comparing the performance of CuO dispersive media for O2 capturing in Liquid Argon"

Caffer, A. M.*; Pizzi, H. B.*; Passos, D. S.*; Carvalho, M. H.*; dos Santos, C. R. A.*; Correia, D.*; Demolin, F.*; Alegre, T. P. M.*; Machado, A. A.*; Segreto, E.*; Adriano, C.*; Pagliuso, P. G.*; Mazali, I. O.*; Soccol, R.*; Bianchi, P.*; Noriler, D.*; et al.

In this work, we have explored the potential of oxygen capture in Liquid Argon (LAr) of the innovative CuO dispersive layered double hydroxide media (R-LDH) and the Ce-doped R-LDH. Low-temperature experiments in the LAr Purification Cryostat (PuLArC) at IFGW/Unicamp were performed using LAr circulation through two filters, one containing the R-LDH (or the Ce-doped R-LDH) material and the other the BASF commercial copper material (Cu-02265 - proposed as a reference O2 getter media by Fermilab) for comparison. Interestingly, the experiments performed in PuLArC revealed that the R-LDH and Ce-doped R-LDH innovative media were capable of capturing O2 from recirculating LAr in PuLArC. For instance, the R-LDH media reduced the O2 contaminants concentration by 80% of its initial values after 200 min of LAr circulation. As for the reference media BASF Cu-S0226, this media reduced the O2 concentration by 40% of its initial value in the same time window. The performance/kg of the studied media will be compared and we will discuss the putative higher potential of the innovative Ce-doped and pure R-LDH media for O2 capturing in LAr which may invoke further tests of these media in larger scale LAr cryostats, possibly at Fermilab and CERN.

JOURNAL OF INSTRUMENTATION 20[3], C03043, 2025. DOI: 10.1088/1748-0221/20/03/C03043

[P034-2025] "Cooperative and competitive effects in pH-dependent surface composition of atmospherically relevant organic ions in water"

Marinho, R. R. T.; Björneholm, O.; Mocellin, A.; Gomes, A. H. D.; Öhrwall, G.; Araújo, O. C.; Rocha, T. C. R.; **Brito, N. A. de***

The molecular surface compositions of aerosols can differ considerably from their bulk counterparts, an aspect often overlooked in climate models. This oversight can potentially affect our understanding of the complex interplay between composition, optical characteristics, and their influence on cloud formation and properties. A substantial portion of aerosol mass often includes organic compounds, such as carboxylic acids and alkyl amines.These organic compounds are surface-active and influence surface tension, an important aspect of cloud droplet activation. To better understand the impact of complex organic mixtures on aerosol surfaces,

we report a liquid-jet X-ray photoelectron spectroscopy (XPS) study exploring the pH-dependent surface composition of aqueous solutions of butyric acid and butylamine, both isolated and mixed. Our findings reveal that the surface composition is highly influenced by the ratio between these solutes and their total surface concentration. Around pH 7, where both solutes are charged, the mixed solution demonstrates cooperative surface behavior, leading to an increased presence of organics at the surface. At extreme pH values, where one solute is charged and the other remains neutral, the solutes act independently, with the neutral species dominating the surface enrichment. We also discuss the molecular mechanisms driving these interactions and their broader implications for aerosol behavior in climate models.

PHYSICAL CHEMISTRY CHEMICAL PHYSICS 27[11], p. 5791-5797, 2025. DOI: 10.1039/d4cp04287e

[P035-2025] "Electrical Manipulation of Intervalley Trions in Twisted MoSe2 Homobilayers at Room Temperature"

Rosa, B. L. T.*; Faria, P. E. Cadore, A. R.; Yang, Y. H.; Koulas-Simos, A.; Palekar, C. C.; Tongay, S. A.; Fabian, J.; Reitzenstein, S.

The impressive physics and applications of intra- and interlayer excitons in a transition metal dichalcogenide twisted-bilayer make these systems compelling platforms for exploring the manipulation of their optoelectronic properties through electrical fields. This work studies the electrical control of excitonic complexes in twisted MoSe2 homobilayer devices at room temperature. Gate-dependent micro-photoluminescence spectroscopy reveals an energy tunability of several meVs originating from the emission of excitonic complexes. Furthermore, this study investigates the twist-angle dependence of valley properties by fabricating devices with stacking angles of theta similar to 1 degrees, theta similar to 4 degrees and theta similar to 18 degrees. Strengthened by density functional theory calculations, the results suggest that, depending on the twist angle, the conduction band minima and hybridized states at the Q-point promote the formation of intervalley hybrid trions involving the Q-and K-points in the conduction band and the K-point in the valence band. By revealing the gate control of exciton species in twisted homobilayers, these findings open new avenues for engineering multifunctional optoelectronic devices based on ultrathin semiconducting systems.

ADVANCED PHYSICS RESEARCH DOI: 10.1002/apxr.202400135 Acesso antecipado: 2025 FEB 9

[P036-2025] "Engineering two-dimensional supramolecular self-assembly: The role of Cl atoms"

Ceccatto, A.*; Campi, G. R.; **Diaz, V. C.*; Ferreira, E. B. D.***; Waleska-Wellnhofer, N. J.; Freiberger, E. M.; Jaekel, S.; Papp, C.; Steinrück, H. P. Mowbray, D. J.; **Siervo, A. de***

On-surface synthesis is a powerful tool for engineering two-dimensional (2D) organic nanostructures by controlling intermolecular interactions between the building blocks. Herein, we explore the role of Cl adatoms in the synthesis and characterization of self-assembled 1,3,5-tris[4-(pyridin)-[1,1'-biphenyl] benzene (TPyPPB) networks on Ag(111), by combining scanning tunneling microscopy (STM), X-ray photoelectron spectroscopy (XPS), and density functional theory (DFT). In the absence of Cl, upon deposition at room temperature (RT), TPyPPB molecules form a highly ordered porous supramolecular network with triangular packing, stabilized by hydrogen bonds (N--H). In the presence of Cl adatoms, sublimated onto the surface using dichloro-(1,10phenanthrolin)-platin(II) (Cl2PhPt) a second molecular precursor, we observe a so-called mixed phase or inverted packing, depending on the applied growth procedure. The mixed phase is characterized by a nonperiodic structure stabilized by intermolecular interactions between TPyPPB, Cl-2PhPt, and Cl. In contrast, when only Cl adatoms and TPyPPB are present on the Ag(111) surface, a non-porous supramolecular arrangement is obtained, stabilized by C-H--Cl hydrogen bonds.

FLATCHEM 50, 100808, 2025. DOI: 10.1016/j.flatc.2025.100808

[P037-2025] "Enhanced Elastocaloric Effects in γ-Graphyne"

Kanegae, G. B.*; Pereira Junior, M. L.; **Galvao, D. S.***; Ribeiro Junior, L. A.; **Fonseca, A. F.***

The global emphasis on sustainable technologies has become a paramount concern for nations worldwide. Specifically, numerous sustainable methods are being explored as promising alternatives to the well-established vapor-compression technologies in cooling and heating devices. One such avenue gaining traction within the scientific community is the elastocaloric (eC) effect. This phenomenon holds promise for efficient cooling and heating processes without causing environmental harm. Studies carried out at the nanoscale have demonstrated the efficiency of the eC effect, proving to be comparable to that of state-of-the-art macroscopic systems. In this study, we used classical molecular dynamics simulations to investigate the elastocaloric effect for the recently synthesized gamma-graphyne. Our analysis goes beyond obtaining changes in eC temperature and the coefficient of performance (COP) for two species of gamma-graphyne nanoribbons (armchair and zigzag). We also explore their dependence on various conditions, including whether they are deposited on a substrate or prestrained. Our findings reveal a substantial enhancement in the elastocaloric effect for gamma-graphyne nanoribbons when subjected to prestrain, amplifying it by at least 1 order of magnitude. Under certain conditions, the changes in the eC temperature and the COP of the structures reach expressive values as high as 224 K and 14, respectively. We discuss the implications of these results by examining the shape and behavior of the carbon-carbon bond lengths within the structures.

ACS APPLIED MATERIALS & INTERFACES 17[9], 13074-13082, 2025. DOI: 10.1021/acsami.4c03302

[P038-2025] "Evaluation of Antibacterial Activity of Bismuth Ferrites Nanoparticles in the Inhibition of E. Coli and S. Aureus Bacteria"

Pancotti, A.; Souza, M. V. de B.; Abreu, A. S.; Rezende, S. R.; Moreli, M. L.; Otero, E. U.; **Landers, R.***; Soares, R.; Wang, J.

In this work, bismuth ferrites (BFO) nanoparticles were produced in the form of using sol-gel technique, followed by annealing in a tube furnace in temperatures from 400 degrees C to 650 degrees C. X-ray diffraction (XRD) results showed the formation of small sizes nanoparticles (NPs) with high purity. Structural analysis displayed that annealing at 600 degrees C could make BFO NPs be fitted to rhombohedral space group (R3c), with small quantity of spurious phases. The sizes of the BFO nanoparticles determined by transmission electron microscopy (HRTEM) are between 50 to 100 nm. To evaluate the efficiency of BFO in antimicrobial susceptibility tests, the nanoparticles were dispersed through cand tested agar diffusion method and dilution in a 96 well plate using a Gram-positive strains (Staphylococcus aureus) and Gram negative strain (Escherichia coli). The antibacterial activity of the BFO NPs was tested at concentrations of 2 mg/mL with MIC greater than 60 mu g/mL for both bacteria.

CHEMISTRY & BIODIVERSITY 22[1], e202402048, 2025. DOI: 10.1002/cbdv.202402048

[P039-2025] "Exact solutions of the Kuramoto model with asymmetric higher order interactions of arbitrary order"

Costa, G. S.; **Novaes, M.*; Aguiar, M. A. M. de***

Higher order interactions can lead to new equilibrium states and bifurcations in systems of coupled oscillators described by the Kuramoto model. However, even in the simplest case of 3-body interactions there are more than one possible functional forms, depending on how exactly the bodies are coupled. Which of these forms is better suited to describe the dynamics of the oscillators depends on the specific system under consideration. Here we show that, for a particular class of interactions, reduced equations for the Kuramoto order parameter can be derived for arbitrarily many bodies. Moreover, the contribution of a given term to the reduced equation does not depend on its order, but on a certain effective order, that we define. We give explicit examples where bi and tri-stability is found and discuss a few exotic cases where synchronization happens via a third order phase transition.

CHAOS SOLITONS & FRACTALS 195, 116243, 2025. DOI: 10.1016/j.chaos.2025.116243

[P040-2025] "High photon-phonon pair generation rate in a two-dimensional optomechanical crystal"

Mayor, F. M.: Malik, S.; **Primo, A. G.***; Gyger, S.; Jiang, W. T.; **Alegre, T. P. M.***; Safavi-Naeini, A. H.

Integrated optomechanical systems are a leading platform for manipulating, sensing, and distributing quantum information, but are limited by residual optical heating. Here, we demonstrate a two-dimensional optomechanical crystal (OMC) geometry with increased thermal anchoring and a mechanical mode at 7.4 GHz, well aligned with the operation range of cryogenic microwave hardware and piezoelectric transducers. The eight times better thermalization than current one-dimensional OMCs, large optomechanical coupling rates, g(0)/2 pi approximate to 880 kHz, and high optical quality factors, Q(opt) = 2.4 x 10(5), allow ground-state cooling (n(m) = 0.32) of the acoustic mode from 3 K and entering the optomechanical strong-coupling regime. In pulsed sideband asymmetry measurements, we show ground-state operation (n(m) < 0.45) at temperatures below 10 mK, with repetition rates up to 3 MHz, generating photon-phonon pairs at approximate to 147 kHz. Our results extend optomechanical system capabilities and establish a robust foundation for future microwave--to-optical transducers with entanglement rates exceeding state-of-the-art superconducting qubit decoherence rates.

NATURE COMMUNICATIONS 16[1], 2576, 2025. DOI: 10.1038/s41467-025-57948-7

[P041-2025] "Impedimetric multi-sensor system with gold and silver nanoparticles applied for basic taste assessment compared with human threshold method sensory analysis"

Raj, D. R. K.; **Gonsalves, M. H.*;** Medeiros, A. C. de; Bolini, H. M. A.; **Riul Jr, A.*;** Barbin, D. F.

Threshold determination forms an integral part of sensory and consumer studies applied for product control and development. The authors examined the potential of an impedimetric electronic tongue to discriminate basic tastes and consider limitations pertaining to the sensory evaluation process. Three samples at lower, medium, and higher concentration levels of basic taste compounds were prepared and subjected to consumer studies (n = 60) using the difference from-control (DFC) test. Simultaneously, all basic tastes were subjected to electronic tongue measurements. The incorporation of nanoparticles increased the overall sensitivity of the electrodes that were examined using the PCA biplot. Results confirmed the efficiency of an electronic tongue in classifying basic tastes, with higher prediction sensitivity of about 99-100 % in non-electrolytic rich compounds such as caffeine, tannic acid, and sucrose. The values dipped among electrolytic compounds such as sodium chloride, monosodium glutamate, and citric acid, which require further investigation. In conclusion, the increased sensitivity to non-electrolytes supports the versatility and economical importance an impedimetric electronic tongue can present for food and pharmaceutical applications.

FOOD CHEMISTRY 472, 142859, 2025. DOI: 10.1016/j.foodchem.2025.142859

[P042-2025] "Investigating Λ baryon production in p-Pb collisions in jets and the underlying event using angular correlations"

Acharya, S.; Adamová, D.; Agarwal, A.; **Chinellato, D. D.*; Guardiano, G. G.*; Liveraro, G. S. S.*; Takahashi, J.*;** et al. ALICE Collaboration

First measurements of hadron- Lambda(h-Lambda) azimuthal angular correlations in p-Pb collisions at root s(NN) = 5.02 TeV using the ALICE detector at the Large Hadron Collider are presented. These correlations are used to separate the production of associated Lambda baryons into three different kinematic regions, namely those produced in the direction of the trigger particle (near side), those produced in the opposite direction (away side), and those whose production is uncorrelated with the jet axis (underlying event). The per-trigger associated Lambda yields in these regions are extracted, along with the near- and away-side azimuthal peak widths, and the results are studied as a function of associated particle pT and event multiplicity. Comparisons with the DPMJET event generator and previous measurements of the phi(1020) meson are also made. The final results indicate that strangeness production in the highest multiplicity p-Pb collisions is enhanced relative to low multiplicity collisions in both the jetlike regions and the underlying event. The production of Lambda relative to charged hadrons is also enhanced in the underlying event when compared to the jetlike regions. Additionally, the results hint that strange quark production in the away-side of the jet is modified by soft interactions with the underlying event.

PHYSICAL REVIEW C 111[1], 015201, 2025. DOI: 10.1103/PhysRevC.111.015201

[P043-2025] "Lattice thermal conductivity of 8-16-4(sun)--graphyne from reverse nonequilibrium molecular dynamics simulations"

Felix, I. M.; Tromer, R. M.; Machado, L. D.; **Galvao, D. S.***; Ribeiro Jr, L. A.; Pereira, M. L.

The thermal conductivity of two-dimensional (2D) materials is critical in determining their suitability for several applications, from electronics to thermal management. In this study, we have used Molecular Dynamics (MD) simulations to investigate the thermal conductivity and phononic properties of 8-16-4(Sun)-Graphyne, a recently proposed 2D carbon allotrope. The thermal conductivity was estimated using reverse non-equilibrium MD simulations following the M & uuml;ller--Plathe approach, revealing a strong dependence on system size. Phonon dispersion calculations confirm the stability of Sun-GY while also showing a significant decrease in thermal conductivity compared to graphene. This decrease is attributed to acetylenic bonds, which enhance phonon scattering. Spectral analysis further revealed that Sun-GY exhibits lower phonon group velocities and increased phonon scattering,

mainly due to interactions between acoustic and optical modes. Sun-GY presents an intrinsic thermal conductivity of approximately 24.6 W/mK, much lower than graphene, making it a promising candidate for applications that require materials with reduced thermal transport properties.

INTERNATIONAL JOURNAL OF HEAT AND MASS TRANSFER 241, 126746, 2025. DOI: 10.1016/j.ijheatmasstransfer.2025.126746

[P044-2025] "Lighting up the structure and electronic properties of α-, ß-, γ-Ag2WO4 polymorphs under laser irradiation: a DFT investigation"

Cabral, L.*; Longo, E.; San-Miguel, M. A.; Leite, E.; **Silva, E. Z. da***; Andres, J.

Laser irradiation (LI)-matter interaction provides a versatile means to manipulate the physicochemical properties of materials. Understanding material responses to LI was the initial driving force for studying the effects of this interaction in solids, but the associated induced dynamics is hindered by the macroscopic number of particles interacting collectively with photonic modes. In this work, we conduct comprehensive theoretical calculations to gain insights into the changes in the lattice structure and electronic properties of alpha-, beta-, gamma-Ag2WO4 polymorphs induced by LI using density functional theory (DFT) calculations based on the electronic temperature (Te) within a two-temperature model (TTM) and ab initio molecular dynamics (AIMD) simulations. Overall, we reveal a clear visualization of how Te induces a structural and electronic transformation process during LI. The analysis of the evolution of the pair correlation function confirms that these polymorphs undergo a transition from crystalline to an amorphous structure under strong electronic excitations with concomitant formation of Ag nanoclusters. These results suggest the critical role that the Ag metallic nanoparticles may play in defining the behavior and properties of these materials. Our results offer physical insights into the thermodynamic stability and electronic properties of laser-irradiated Ag2WO4 polymorphs, which can inform on structural details currently inaccessible to experimental techniques. The presented approach is a versatile and sensitive tool for studying defect distribution and clustering processes in other functional Ag-based semiconductors.

PHYSICAL CHEMISTRY CHEMICAL PHYSICS 27[14], p. 6836-6844, 2025. DOI: 10.1039/d4cp04349a

[P045-2025] "Measurement of 3ΛH production in Pb-Pb collisions at √sNN=5.02 TeV"

Acharya, S.; Adamová, D.; Agarwal, A.; **Chinellato, D. D.*; Guardiano, G. G.*; Liveraro, G. S. S.*; Takahashi, J.*;** et al.
ALICE Collaboration

The first measurement of H-3(Lambda) and 3/Lambda(H) over bar differential production with respect to transverse momentum and centrality in Pb-Pb collisions at root(NN)--N-S = 5.02 TeV is presented. The H-3(Lambda) has been reconstructed via its two-charged-body decay channel, i.e., H-3(Lambda) -> He-3 + pi(-). A Blast-Wave model fit of the..T--differential spectra of all nuclear species measured by the ALICE collaboration suggests that the H-3(Lambda) kinetic freeze-out surface is consistent with that of other nuclei. The ratio between the integrated yields of H-3(Lambda) and He-3(Lambda) is compared to predictions from the statistical hadronisation model and the coalescence model, with the latter being favoured by the presented measurements.

PHYSICS LETTERS B 860, 2025. DOI: 10.1016/j.physletb.2024.139066

[P046-2025] "Measurement of inclusive and differential cross sections for W+W- production in proton-proton collisions at √s=13.6 TeV"

Hayrapetyan, A.; Tumasyan, A.; Adam, W.; **Chinellato, J. A.***; et al.
CMS Collaboration

Measurements at root s = 13.6 TeV of the opposite-sign W boson pair production cross section in proton-proton collisions are presented. The data used in this study were collected with the CMS detector at the CERN LHC in 2022, and correspond to an integrated luminosity of 34.8 fb(-1). Events are selected by requiring one electron and one muon of opposite charge. A maximum likelihood fit is performed on signal- and background-enriched data categories dfined by the flavor and charge of the leptons, the number of jets, and number of jets originating from b quarks. The overall sensitivity is significantly better than that of previous results with a similar integrated luminosity. The improvement comes from a more rfined control of experimental uncertainties and an improved fit strategy. An inclusive W+W- production cross section of 125.7 +/- 5.6 pb is measured, in agreement with standard model predictions. Cross sections are also reported in a fiducial region close to that of the detector acceptance, both inclusively and differentially, as a function of the jet multiplicity in the event. For the first time in proton-proton collisions, WWevents with zero, one, and at least two jets are studied simultaneously and compared with recent theoretical predictions.

PHYSICS LETTERS B 861, 139231, 2025. DOI: 10.1016/j.physletb.2024.139231

[P047-2025] "Measurement of the depth of maximum of air--shower profiles with energies between 1018.5 and 1020 eV using the surface detector of the Pierre Auger Observatory and deep learning"

Halim, A. A.; Abreu, P.; Aglietta, M.; **Arbeletche, L. B.*; Chinellato, J. A.*; Dobrigkeit, C.*; Fauth, A. C.*; Payeras, A. M.*; Akim, J. V. R.***; et al.
Pierre Auger Collaboration

We report an investigation of the mass composition of cosmic rays with energies from 3 to 100 EeV (1 EeV = 10(18) eV) using the distributions of the depth of shower maximum X--max. The analysis relies on similar to 50; 000 events recorded by the surface detector of the Pierre Auger Observatory and a deep-learning-based reconstruction algorithm. Above energies of 5 EeV, the dataset offers a 10-fold increase in statistics with respect to fluorescence measurements at the Observatory. After cross-calibration using the fluorescence detector, this enables the first measurement of the evolution of the mean and the standard deviation of the X-max distributions up to 100 EeV. Our findings are threefold: (i) The evolution of the mean logarithmic mass toward a heavier composition with increasing energy can be confirmed and is extended to 100 EeV. (ii) The evolution of the fluctuations of X-max toward a heavier and purer composition with increasing energy can be confirmed with high statistics. We report a rather heavy composition and small fluctuations in X-max at the highest energies. (iii) We find indications for a characteristic structure beyond a constant change in the mean logarithmic mass, featuring three breaks that are observed in proximity to the ankle, instep, and suppression features in the energy spectrum.

PHYSICAL REVIEW D 111[2], 022003, 2025. DOI: 10.1103/PhysRevD.111.022003

[P048-2025] "Melanin/PEDOT:PSS organic synaptic transistors: a step towards sustainable neuromorphic applications"

Nozella, N. L.; **Selmi, G. S.*;** Guerra, N. B.; Piton, M. R.; Graeff, C. F. O.; **Oliveira, R. F. de***

Inspired by the functioning of the human brain, organic synaptic transistors represent a promising avenue for developing neuromorphic technologies. However, achieving sustainability while maintaining performance and functionality remains a critical challenge. Here, we report on an innovative strategy where synthetic melanin (Mel)-a natural pigment known for its improved ionic-electronic coupling, high volumetric capacitance, and environmentally friendly characteristics-is blended with benchmark poly(3,4-ethylenedioxythiophene) polystyrene sulfonate (PEDOT:PSS) to fabricate synaptic transistors. Mel/PEDOT:PSS blends having different amounts of Mel have been systematically evaluated as semiconducting layer in organic electrochemical transistors. Our findings reveal that Mel incorporation at different concentrations enables tunable synaptic responses, such as enhanced memory retention and access to multiple memory states. These effects arise from the unique properties of Mel which modulate the charge density of PEDOT:PSS in a controlled manner. This approach demonstrates the potential for developing highly stable, multi--level memory materials for organic neuromorphic devices while addressing sustainability goals. We believe our strategy can open new avenues via the integration of natural and bio-inspired materials into organic semiconductors towards the development of sustainable neuromorphic technologies.

NEUROMORPHIC COMPUTING AND ENGINEERING 5[1], 014014, 2025. DOI: 10.1088/2634-4386/adbccd

[P049-2025] "Multiplicity dependence of Γ production at forward rapidity in pp collisions at √s=13 TeV"

Acharya, S.; Adamová, D.; Adler, A.; **Chinellato, D. D.*; Guardiano, G. G.*; Jahnke, C.*; Takahashi, J.***; et al.
ALICE Collaboration

The measurement of Gamma(1S), Gamma(2S), and Gamma(3S) yields as a function of the charged-particle multiplicity density, dN(ch)/d eta, using the ALICE experiment at the LHC, is reported in pp collisions at root s = 13 TeV. The Gamma meson yields are measured at forward rapidity (2.5 < y < 4) in the dimuon decay channel, whereas the charged-particle multiplicity is defined at central rapidity (vertical bar eta vertical bar < 1). Both quantities are divided by their average value in minimum bias events to compute the self-normalized quantities. The increase of the self-normalized Gamma(1S), Gamma(2S), and Gamma(3S) yields is found to be compatible with a linear scaling with the self-normalized dN(ch)/d eta, within the uncertainties. The self-normalized yield ratios of excited-to-ground Gamma states are compatible with unity within uncertainties. Similarly, the measured double ratio of the self-normalized Gamma(1S) to the self-normalized J/psi yields, both measured at forward rapidity, is compatible with unity for self-normalized charged-particle multiplicities beyond one. The measurements are compared with theoretical predictions incorporating initial or final state effects.

NUCLEAR PHYSICS B 1011[116786, 2025. DOI: 10.1016/j.nuclphysb.2024.116786

[P050-2025] "Non-standard interactions of supernova neutrinos and mass ordering ambiguity at DUNE"

Jana, S.; **Porto, Y.***

We show that non-standard neutrino interactions (NSI) can notably modify the pattern of resonant flavor conversion of neutrinos within supernovae and significantly impact the neutronization burst signal in forthcoming experiments such as the Deep Underground Neutrino Experiment (DUNE). The presence of NSI can invert the energy levels of neutrino matter eigenstates and even induce a new resonance in the inner parts close to the protoneutron star. We demonstrate how DUNE can use these new configurations of energy levels to have sensitivity to NSIs down to O(0.1). We also elucidate how the effect may result in a puzzling confusion of normal and inverted mass orderings by highlighting the emergence or vanishing of the neutronization peak, which distinguishes between the two mass orderings. Potential implications are analyzed thoroughly.

JOURNAL OF COSMOLOGY AND ASTROPARTICLE PHYSICS [3], 046, 2025. DOI: 10.1088/1475-7516/2025/03/046

[P051-2025] "On-Surface Synthesis of 1D and 2D Porphyrin Metal-Organic Networks on Ag(100) Tuned by Substrate Temperature"

Herrera-Reinoza, N.*; Mowbray, D. J.; Paz, A. P.; **Santos, A. C. dos*; Ferreira, R. C. D.*; Siervo, A. de***

The production of single-layer polymer ribbons and sheets composed of fused porphyrin rings, named porphene, an analog to graphene, has been aimed over the years as a promising material for applications. Several attempts to polymerize porphyrin rings have used the Ullmann-coupling reaction among the different synthesis routes. In this paper, we report the on-surface synthesis of organometallic molecular chains (1D) and porous networks (2D) from the free-base 5,10,15,20-tetrakis(4-bromophenyl)-porphyrin (H2TBrPP) on Ag(100). We investigated the adsorption of H2TBrPP using a comprehensive multitechnique approach combining scanning tunneling microscopy (STM) and X-ray photoelectron spectroscopy (XPS), with density functional theory (DFT) based calculations. We find that distinct thermal stimuli applied to the substrate during the deposition lead to different final nanostructures (1D and 2D). This shows an evident thermal selectivity related to porphyrin conformation and substrate interaction, revealing different activation energies. Free-based porphyrins are shown to adopt the so-called "inverted" conformation on Ag(100), which was previously reported exclusively on the Cu(111) surface. Here, we explain the coexistence of these two porphyrins' molecular conformations ("inverted" versus "saddle"). Moreover, based on DFT calculations, we propose a mechanism to overcome the kinetically trapped intermediate organometallic state to allow complete C-C coupling during the Ullmann reaction of porphyrin ring derivatives.

JOURNAL OF PHYSICAL CHEMISTRY C, 2025. DOI: 10.1021/acs.jpcc.4c08308 **Early Access Date: MAR 2025**

[P052-2025] "Optical Memory in a MoSe2/Clinochlore Device"

Ames, A.; Sousa, F. B.; Souza, G. A. D.; **Rodrigues, G.***

Two-dimensional heterostructures have been crucial in advancing optoelectronic devices utilizing van der Waals materials. Semiconducting transition-metal dichalcogenide monolayers, known for their unique optical properties, offer extensive possibilities for light-emitting devices. Recently, a memory-driven optical device, termed a Mem-emitter, was proposed by using these monolayers atop dielectric substrates. The successful realization of such devices heavily depends on the selection of the optimal substrate. Here, we report a pronounced memory effect in a MoSe2/clinochlore device, evidenced by an electric hysteresis in the intensity and energy of MoSe2 monolayer emissions. This demonstrates both population- and transition-rate-driven Mem-emitter abilities. Our theoretical approach correlates these memory effects with internal state variables of the substrate, emphasizing that a clinochlore-layered structure is crucial for a robust and rich memory response. Tipo de documento: Article

This work introduces a novel two-dimensional device with promising applications in memory functionalities, highlighting the importance of alternate insulators in the fabrication of van der Waals heterostructures.

ACS APPLIED MATERIALS & INTERFACES 17[8], p. 12818-12826, 2025. DOI: 10.1021/acsami.4c19337

[P053-2025] "Optical properties of MnTe2 few-layer quantum dots"

Ninan, G. G.; Varghese, M.; Gowda, C. C.; **Tromer, R.* Galvao, D. S.***

Quantum dots (QDs) are gaining attention as a possible emissive material that might be used in flexible optoelectronic and photonic systems. In the present work, the temperature--dependent photoluminescence (TDPL) property of manganese di-telluride (MnTe2) QDs was investigated. The room-temperature PL is attributed to the abrupt breakage of the large-area MnTe2 nanosheets by ultrasonication, which integrates defect--mediated localized trap states inside the electronic bandgap. As a result, deliberately generated defect states ultimately generate such PL emission of QDs. Density functional theory (DFT) results further validate the experimental interpretations of the origin of TDPL. In addition, through an in-situ liquid diffusion approach, the QDs were also integrated into a NaCl matrix. Due to light scattering properties, the hybrid crystals exhibit fluorescence centres at various excitation wavelengths. These results suggest that these MnTe2 QDs can be used as an effective basis for future flexible optoelectronic applications.

OPTICAL MATERIALS 159, 116619, 2025. DOI: 10.1016/j.optmat.2024.116619

[P054-2025] "Optomechanical microgear cavity"

Zurita, R. O.*; Kersul, C. M.*; Schilder, N. J.*; Wiederhecker, G. S.*; Alegre, T. P. M.*

We introduce a novel optomechanical microgear cavity for both optical and mechanical isotropic materials, featuring a single-etch configuration. The design leverages a conjunction of phononic and photonic crystal-like structures to achieve remarkable confinement of both optical and mechanical fields. The microgear cavity we designed in amorphous silicon nitride exhibits a mechanical resonance at 4.8 GHz, and whispering gallery modes in the near-infrared, with scattering--limited quality factors above the reported material limit of up to 107. Notably, the optomechanical photoelastic overlap contribution reaches 75% of the ideal configuration seen in a floating ring structure. (c) 2024 Optica Publishing Group. All rights, including for text and data mining (TDM), Artificial Intelligence (AI) training, and similar technologies, are reserved.

JOURNAL OF THE OPTICAL SOCIETY OF AMERICA B-OPTICAL PHYSICS 42[1], p. 1-6, 2025. DOI: 10.1364/JOSAB.543899

[P055-2025] "Particle production as a function of charged--particle flattenicity in pp collisions at √s=13TeV"

Acharya, S.; Adamová, D.; Agarwal, A.; **Chinellato, D. D.*; Guardiano, G. G.*; Liveraro, G. S. S.*; Takahashi, J.*;** et al. ALICE Collaboration

This paper reports the first measurement of the transverse momentum (p(T)) spectra of primary charged pions, kaons, (anti)protons, and unidentified particles as a function of the charged-particle flattenicity in pp collisions at root s = 13 TeV. Flattenicity is a novel event shape observable that is measured in the pseudorapidity intervals covered by the V0 detector, 2.8 < eta < 5.1 and -3.7 < eta < -1.7. According to QCD-inspired phenomenological models, it shows sensitivity to multiparton interactions and is less affected by biases toward larger p(T) due to local multiplicity fluctuations in the V0 acceptance than multiplicity. The analysis is performed in minimum-bias (MB) as well as in high-multiplicity events up to p(T) = 20 GeV/c. The event selection requires at least one charged particle produced in the pseudorapidity interval vertical bar eta vertical bar < 1. The measured p(T) distributions, average p(T), kaon-to-pion and proton-to-pion particle ratios, presented in this paper, are compared to model calculations using PYTHIA 8 based on color strings and EPOS LHC. The modification of the p(T)-spectral shapes in low-flattenicity events that have large event activity with respect to those measured in MB events develops a pronounced peak at intermediate p(T) (2 < p(T) < 8 GeV/c), and approaches the vicinity of unity at higher p(T). The results are qualitatively described by PYTHIA, and they show different behavior than those measured as a function of charged-particle multiplicity based on the V0M estimator.

PHYSICAL REVIEW D 111[1], 012010, 2025. DOI: 10.1103/PhysRevD.111.012010

[P056-2025] "Particle production by γ-γ interactions in future electron-ion colliders"

Bertulani, C. A; **Francener, R.***; Gonçalves, V. P.; Souza, J. T. de;

The particle production in photon-photon (gamma gamma) interactions present in electron-ion collisions is investigated. We present calculations for the total cross sections and event rates related to the production of light mesons [eta, eta', f0 and f2], charmonium [eta c and chi c], and charmoniumlike [X (3915),X (3940),X (4140), and X (6900)] states, considering the Electron - Ion Collider, Electron - ion collider in China, Large Hadron electron Collider, and Future Circular Collider - electron hadron energies. Our predictions demonstrate that experimental studies of these processes are feasible and useful to constrain the properties of light mesons and quarkonium states and shed some light on the configuration of the considered charmoniumlike states.

PHYSICAL REVIEW C 111[2], 025201, 2025. DOI: 10.1103/PhysRevC.111.025201

[P057-2025] "Results of a Geant4 benchmarking study for bio-medical applications, performed with the G4-Med system"

Arce, P.; Archer, J. W.; Arsini, L.; **Tomal, A.*;** et al.

BackgroundGeant4, a Monte Carlo Simulation Toolkit extensively used in bio-medical physics, is in continuous evolution to include newest research findings to improve its accuracy and to respond to the evolving needs of a very diverse user community. In 2014, the G4-Med benchmarking system was born from the effort of the Geant4 Medical Simulation Benchmarking Group, to benchmark and monitor the evolution of Geant4 for medical physics applications. The G4-Med system was first described in our Medical Physics Special Report published in 2021. Results of the tests were reported for Geant4 10.5.PurposeIn this work, we describe the evolution of the G4-Med benchmarking system. MethodsThe G4-Med benchmarking suite currently includes 23 tests, which benchmark Geant4 from the calculation of basic physical quantities to the simulation of more clinically relevant set-ups. New tests concern the benchmarking of Geant4-DNA physics and chemistry components for regression testing purposes, dosimetry for brachytherapy with a 125I$<^>{125}I$ source, dosimetry for external x-ray and electron FLASH radiotherapy,

experimental microdosimetry for proton therapy, and in vivo PET for carbon and oxygen beams. Regression testing has been performed between Geant4 10.5 and 11.1. Finally, a simple Geant4 simulation has been developed and used to compare Geant4 EM physics constructors and physics lists in terms of execution times.ResultsIn summary, our EM tests show that the parameters of the multiple scattering in the Geant4 EM constructor G4EmStandardPhysics_option3 in Geant4 11.1, while improving the modeling of the electron backscattering in high atomic number targets, are not adequate for dosimetry for clinical x-ray and electron beams. Therefore, these parameters have been reverted back to those of Geant4 10.5 in Geant4 11.2.1. The x-ray radiotherapy test shows significant differences in the modeling of the bremsstrahlung process, especially between G4EmPenelopePhysics and the other constructors under study (G4EmLivermorePhysics, G4EmStandardPhysics_option3, and G4EmStandardPhysics_option4). These differences will be studied in an in-depth investigation within our Group. Improvement in Geant4 11.1 has been observed for the modeling of the proton and carbon ion Bragg peak with energies of clinical interest, thanks to the adoption of ICRU90 to calculate the low energy proton stopping powers in water and of the Linhard-Sorensen ion model, available in Geant4 since version 11.0. Nuclear fragmentation tests of interest for carbon ion therapy show differences between Geant4 10.5 and 11.1 in terms of fragment yields. In particular, a higher production of boron fragments is observed with Geant4 11.1, leading to a better agreement with reference data for this fragment.ConclusionsBased on the overall results of our tests, we recommend to use G4EmStandardPhysics_option4 as EM constructor and QGSP_BIC_HP with G4EmStandardPhysics_option4, for hadrontherapy applications. The Geant4--DNA physics lists report differences in modeling electron interactions in water, however, the tests have a pure regression testing purpose so no recommendation can be formulated.

MEDICAL PHYSICS, 2025. DOI: 10.1002/mp.17678. **Early Access: 2025 FEB 21**

[P058-2025] "Search for a standard model-like Higgs boson in the mass range between 70 and 110 GeV in the diphoton final state in proton-proton collisions at √s=13 TeV"

Hayrapetyan, A.; Tumasyan, A.; Adam, W.; **Chinellato, J. A.*;** et al.
CMS Collaboration

The results of a search for a standard model-like Higgs boson decaying into two photons in the mass range between 70 and 110 GeV are presented. The analysis uses the data set collected by the CMS experiment in proton-proton collisions at root s = 13 TeV corresponding to integrated luminosities of 36.3 fb(-1), 41.5 fb(-1) and 54.4 fb(-1) during the 2016, 2017, and 2018 LHC running periods, respectively. No significant excess over the background expectation is observed and 95% cofidence level upper limits are set on the product of the cross section and branching fraction for decays of an additional Higgs boson into two photons. The maximum deviation with respect to the background is seen for a mass hypothesis of 95.4 GeV with a local (global) significance of 2.9 (1.3) standard deviations. The observed upper limit ranges from 15 to 73 fb.

PHYSICS LETTERS B 860, 139067, 2025. DOI: 10.1016/j.physletb.2024.139067

[P059-2025] "Search for dark matter produced in association with a pair of bottom quarks in proton-proton collisions at √s=13 TeV"

Hayrapetyan, A.; Tumasyan, A.; Adam, W.; **Chinellato, J. A.*;** et al.
CMS Collaboration

A search for dark matter (DM) particles produced in association with bottom quarks is presented. The analysis uses proton-proton collision data at a center-of-mass energy of root s = 13 TeV, corresponding to an integrated luminosity of 138 fb(-1). The search is performed in a final state with large missing transverse momentum and a pair of jets originating from bottom quarks. No significant excess of data is observed with respect to the standard model expectation. Results are interpreted in the context of a type-II two-Higgs-doublet model with an additional light pseudoscalar (2HDM+a). An upper limit is set on the mass of the lighter pseudoscalar, probing masses up to 260 GeV at 95% confidence level. Sensitivity to the parameter space with the ratio of the vacuum expectation values of the two Higgs doublets, tan beta, greater than 15 is achieved, capitalizing on the enhancement of couplings between pseudoscalars and bottom quarks with high tan beta.

JOURNAL OF HIGH ENERGY PHYSICS [2], 050, 2025. DOI: 10.1007/JHEP02(2025)050

[P060-2025] "Search for light long-lived particles decaying to displaced jets in proton-proton collisions at √s=13.6TeV"

Hayrapetyan, A.; Tumasyan, A.; Adam, W.; **Chinellato, J. A.*;** et al.
CMS Collaboration

A search for light long-lived particles (LLPs) decaying to displaced jets is presented, using a data sample of proton-proton collisions at a center-of-mass energy of 13.6 TeV, corresponding to an integrated luminosity of 34.7 fb(-1), collected with the CMS detector at the CERN LHC in 2022. Novel trigger, reconstruction, and machine-learning techniques were developed for and employed in this search. After all selections, the observations are consistent with the background predictions. Limits are presented on the branching fraction of the Higgs boson to LLPs that subsequently decay to quark pairs or tau lepton pairs. An improvement by up to a factor of 10 is achieved over previous limits for models with LLP masses smaller than 60 GeV and proper decay lengths smaller than 1 m. The first constraints are placed on the fraternal twin Higgs (FTH) and folded supersymmetry (FSUSY) models, where the lower bounds on the top quark partner mass reach up to 350 GeV for the FTH model and 250 GeV for the FSUSY model.

REPORTS ON PROGRESS IN PHYSICS 88[3], 037801, 2025. DOI: 10.1088/1361-6633/adaa13

[P061-2025] "Synthesis, Characterization, and Application of an Ecofriendly C/TiO2 Composite to Efficiently Remove Reactive Black 5 (RB-5) Textile Dye from Aqueous Solutions"

Paquini, L. D.; Marconsini, L. T.; **Lima, B. S. de***; Profeti, L. P. R.; Ribeiro, J.; Profeti, D.

The textile industry is known for its high water consumption and production of toxic effluents, including azo dyes such as Reactive Black 5 (RB-5), which are resistant to removal. Adsorption offers a promising, cost-effective solution, particularly with value-added composites made from abundant materials. This study synthesized, characterized, and applied a C/TiO2-based composite to remove RB-5 from water. XRD analysis only confirmed anatase as the primary support, while FTIR detected adsorbate molecules on the C/TiO2 surface, marked by the appearance of a sulfone group band. Raman and XPS analyses indicated reduced Sp2 carbon content and lower graphitization after adsorption, probably due to mechanical stress. Additionally, nitrogen physisorption analysis demonstrated that the material is mesoporous, with a surface area of 56.24 m2 g-1, and a pore diameter of 9.41 nm.

The composite exhibited strong affinity for anionic species like RB-5, especially at pH values below the point of zero charge (7.47). Batch studies demonstrated Avrami kinetic adsorption at a rate of 0.3023 min-1 (at 25 degrees C), while temperature effects followed the Arrhenius model, with an activation energy of +41.10 kJ mol-1. Sips isotherm data indicated a maximum adsorption capacity of 17.48 mg g-1 at 55 degrees C. Thermodynamic analysis confirmed an entropically controlled, endothermic, spontaneous process at high temperatures. These aspects confirm the potential of eco-friendly C/TiO2 composite for effective RB-5 removal from aqueous solutions.

ACS OMEGA 10[12], p. 12241-12259, 2025. DOI: 10.1021/acsomega.4c10884

[P062-2025] "The role of the bandgap in photoinduced crystallization of tellurium in Cd1-xMnxTe thin films under visible light irradiation"

Souza, M. A.; **Soares, T. C.***; Ferreira, S. O.; Rodrigues, L. N.; Rizzi, L. G.; Moura, L. G.; Araujo, E. N. D.

We report the role of the bandgap energy in Cd 1-x MnxTe thin films in the photoinduced crystallization of tellurium under prolonged exposure to visible light. Raman spectroscopy was used to quantify the evolution of the trigonal phase of tellurium over time. Our results reveal that when the energy of incident photons exceeds the bandgap energy, the photocrystallization process seems to be controlled by diffusion and consistent with the growth of one-dimensional tellurium forming crystalline structures. Conversely, when the excitation energy is lower than the bandgap energy, the photoinduced effect is completely suppressed. These findings provide valuable insights into how bandgap engineering can be utilized to control material properties in thin film systems, potentially advancing the development of novel semiconductor devices.

JOURNAL OF PHYSICS D-APPLIED PHYSICS 58[16], 165103, 2025. DOI: 10.1088/1361-6463/adb3b7

[P063-2025] "Thermal Dynamics Induced by Surface Acoustic Waves in Lanthanide-Doped Core@Multishell Nanoparticles"

Pinto, P. B.*; Matrone, P. W.*; Ferreira, F. S.; Santos, P. V.; Sigoli, F. A.**; Couto Jr, O. D. D.***

Accurate local temperature readout in integrated nanoscaled devices driven by high-frequency surface acoustic waves (SAWs) has a strong technological interest. The optical response of lanthanide (Ln)-doped NaLnF(4) core@multishell nanoparticles inserted into SAW delay lines is reported. The recombination dynamics between the(2)H(11/2) and S-4(3/2) to the I-4(15/2) states of Er3+ is probed under SAWs modulation at 5, 225, and 290 K. It is shown that the spectral weight of the upconverted individual Stark levels of the S-4(3/2) band changes with the SAW and that their recombination lifetimes decrease as the SAW power is increased. By monitoring the luminescence intensity ratio (LIR), it is shown that such dynamics is consistent with a temperature increase and a carrier repopulation process across the S-4(3/2) Stark levels induced by Joule heating, which can reach up to 47 K at cryogenic temperatures. These effects, however, can be strongly suppressed by reducing the SAW duty cycle during the optical measurements. The results demonstrate that heating of nanoscopic systems integrated into SAW devices can be quite pronounced and that, since they do not interact with the SAW strain or piezoelectric field, these NaLnF(4) nanoparticles can be effectively employed as nanoscale in-situ and in-operando thermometers in such kind of application.

ADVANCED OPTICAL MATERIALS 2403497, 2025. DOI: 10.1002/adom.202403497

[P064-2025] "Wear resistance and conducting property of laser-melted copper-graphene composite"

Das, R.; de Oliveira, R. B.; **Tromer, R.*; Galvao, D. S.***; Owuor, P. S.; Khan, A.; Katiyar, N. K.; Machado, L. D.; Tiwary, C. S.

Additive manufacturing/3D printing is currently utilized to build complex structures, such as heat exchangers. This paper investigates one of the additive manufacturing processes, powder bed fusion melting (PBF-M), with optimized laser power and scan rate to investigate the mechanical, tribological, and electrical properties of copper-graphene (Cu-GR) composite. We have employed a predetermined laser scan path to melt the Cu-GR alloy to improve the aforementioned properties. The microstructural and hardness of the Cu-GR composites have also been compared with PBF-M copper. Among the investigated Cu--GR composites, Cu-1wt%GR exhibits the highest micro-Vickers hardness value. This paper also demonstrates the upper limit to the concentration of GR that can be added as reinforcement to the Cu matrix for successful PBF-M process. Graphene addition to the Cu matrix and their uniform distribution achieved through PBF-M process has significant effect in mechanical and wear properties of the composites. The underlying mechanism of tribological and electrical properties have shown through experiments and Molecular Dynamics simulations, while Density Functional Theory simulations were also used to address the experimentally observed changes in electrical conductivity.

PROGRESS IN ADDITIVE MANUFACTURING, 2025. DOI: 10.1007/s40964-025-01037-0. **Early aceess: 2025 MAR 12**

[P065-2025] "What is "quantum" about quantum gravity?"

Torrieri, G.*

Assuming the validity of the equivalence principle in the quantum regime, we argue that one of the assumptions of the usual definition of quantum mechanics, namely separation between the "classical" detector and the "quantum" system, must be relaxed. We argue, therefore, that if both the equivalence principle and quantum mechanics continue to survive experimental tests, then this favors "informational" interpretations of quantum mechanics (where formalism is built around relations between observables, defined as information that can be accessed by an observer of the system. In particular "collapse" is understood as a change of relative information as the detector interacts with the system) over "ontic ones" (assuming the physical reality of states and wave functions, which are assumed to be more than informational objects. In particular collapse is understood as a physical process). In particular, we show that relational-type interpretations can readily accommodate the equivalence principle via a minor modification of the assumptions used to justify the formalism. We qualitatively speculate what a full generally covariant quantum dynamics could look like, and comment on experimental investigations.

INTERNATIONAL JOURNAL OF MODERN PHYSICS D, 2025. DOI: 10.1142/S0218271825500166. **Early Access: 2025 MAR 11**

***Autores da comunidade IFGW**
Fonte: Web of Science on-line (WOS)

Defesas de Dissertações do IFGW

[D006-2025] "Estudo de Acoplamento Magnético entre Microfios Metálicos e Cavidades 3D Induzido Eletricamente"
Aluno: Ítalo Lambert Soares Andrade
Orientador: Prof. Dr. Francisco Paulo Marques Rouxinol
Data: 20/03/2025

[D007-2025] "Crescimento e caracterização de filmes ultrafinos de ZnS sobre Ag(111)"
Aluno: Iago Aédon Silva Prior
Orientador: Prof. Dr. Abner de Siervo
Data: 28/03/2025

[D008-2025] "Transistores de Filmes Finos para Sinapse Artificial e Aplicações Neuromórficas)"
Aluno: Guilherme Segolin Selmi
Orientador: Prof. Dr. Rafael Furlan de Oliveira
Data: 14/04/2025

Defesas de Teses do IFGW

[T005-2025] "Efeitos coletivos longitudinais em síncrotrons com sistema de rf duplo"
Aluno: Murilo Barbosa Alves
Orientador: Profa. Dra. Liu Lin
Data: 31/03/2025

[T006-2025] "Nanofotônica de óxidos semicondutores de baixa dimensionalidade nas faixas de infravermelho e Terahertz"
Aluno: Rafael Alves Mayer
Orientador: Prof. Dr. Raul de Oliveira Freitas
Data: 09/04/2025

Fonte: Portal IFGW/Eventos
Disponível em: https://portal.ifi.unicamp.br/a-instituicao/eventos/month.calendar/2025/04/16/-

Defesas de Dissertações e Teses do PECIM

***Sem atualização na página no período**
Fonte: Página do PECIM
Disponível em: https://www.pecim.unicamp.br/bancas

Cadastre-se no site do Boletim Abstracta como leitor, e receba os avisos da publicação de novos números por e-mail.

Abstracta

Instituto de Física
Diretor: Profa. Dra. Mônica Alonso Cotta
Diretora Associada: Prof. Dr. Marcos Cesar de Oliveira
Universidade Estadual de Campinas - UNICAMP
Cidade Universitária Zeferino Vaz
13083-859 - Campinas - SP - Brasil
e-mail: secdir@ifi.unicamp.br
Fone: +55 19 3521-5300

Publicação

Biblioteca do Instituto de Física Gleb Wataghin
http://portal.ifi.unicamp.br/biblioteca
Instagram: @bif.unicamp

Diretora Técnica: Sandra Maria Carlos Cartaxo
Coordenadora da Comissão de Biblioteca: Profa. Dra. Arlene Cristina Aguilar

Elaboração e editoração:
Maria Graciele Trevisan (Bibliotecária)
Amelia Galdino Monteiro Amancio (Técnica)

Contato: infobif@ifi.unicamp.br